Does Lower-Stratospheric Shear Influence the Mesoscale Organization of Convection?

Todd P. Lane

School of Earth Sciences and ARC Centre of Excellence for Climate Extremes, The University of Melbourne, Melbourne, Australia

ORCID: 0000-0003-0171-6927

Corresponding author: Todd Lane (tplane@unimelb.edu.au)

Key Points:

- Idealized simulations demonstrate that the mesoscale organization of convection can be affected by lower-stratospheric wind shear
- There is a preference for mesoscale convective systems to propagate in the same direction as the lower-stratospheric wind shear vector
- Results provide insight into a new mechanism for organized convection and stratosphere-troposphere interactions

Key Words:

- Gravity waves
- Organized convection
- Thunderstorms
- Stratosphere-troposphere interaction
- Quasi-Biennial Oscillation (QBO)
- Madden-Julian Oscillation (MJO)

Abstract

Organized mesoscale convection is important for many atmospheric phenomena and hazards, however the understanding of its governing mechanisms is incomplete. Theories explaining mesoscale organization rely on the interaction between convection outflows and lower-tropospheric wind shear. Here a new mechanism is presented, where lower-stratospheric wind shear is shown to influence mesoscale organization. The mechanism is linked to coupling between convection and gravity waves, with the stratosphere playing a role in shaping the tropospheric wave spectrum. The key result is that lower-stratospheric shear creates a preference for organized systems propagating in the same direction as the shear vector by weakening the systems propagating in the opposite direction to the shear. This result has important implications for stratosphere-troposphere interactions, numerical modeling, and understanding of convective organization in general.

Plain Language Summary

Many people think thunderstorms are amazing and numerous scientists spend their lives researching them because they are important for weather and climate. It might therefore be surprising that we don't fully understand how thunderstorms form. We know what's important to make clouds grow, like the way the temperature and water vapour changes with altitude. But something else has to happen to make clouds become thunderstorms. What we typically teach at university is that cold air falls out the bottom of clouds, pushing the near-surface air upwards to make new clouds. If the wind near the surface changes with altitude in just the right way, the new clouds will form thunderstorms. Most meteorologists are happy with this theory, but it doesn't work all the time. Here I use a simplified computer model to show that the wind above the clouds can affect thunderstorm behaviour. The storms create ripples in the wind that travel upwards. Then the wind above the clouds reflects the ripples back downwards where they affect the storms' lifecycle. This is a complex process, and we need to spend more time searching for it in real data and in more complicated computer models to see how often it occurs in the real world.

1 Introduction

Organized mesoscale convection is a key contributor to precipitation, the Earth's energy budget, and meteorological hazards. There has been extensive research on the dynamics of mesoscale organization through observational (e.g., Lemone et al. 1998), theoretical (e.g., Moncrieff 1981), and modeling studies (e.g., Weisman and Rotunno 2004); see Houze (2018) for a recent review. However, organized mesoscale convection remains a deficiency of all models with parameterized convection (e.g., Moncrieff et al. 2017), which underlines the importance of ongoing research into the governing mechanisms.

Most previous work on the mechanisms controlling mesoscale convective systems have focused on the importance of lower-tropospheric wind shear and its interactions with storm outflows in determining the structure and longevity of mesoscale convective systems (MCSs) (e.g., Thorpe et al. 1982, Weisman and Rotunno 2004). Shear in the middle and upper-troposphere is also important (e.g., Parker and Johnson 2000). However, in situations with weaker shear or weaker cold pools, other mechanisms, like gravity waves, can have a prominent impact on MCS dynamics (e.g., Lane and Moncrieff 2015, hereafter LM15; Grant et al. 2018, 2020). In this study, a new paradigm for convective organization is introduced, whereby stratospheric wind shear is shown to influence MCSs through gravity wave-convection interactions.

Studies by Mapes (1993), Lac et al. (2001), Lane and Reeder (2001), Fovell (2002), Tulich and Mapes (2008) and others highlight how tropospheric gravity waves emitted from MCSs destabilize the environment surrounding those systems, promoting upscale growth. Shige and Satomura (2001) and Stechmann and Majda (2009) identified how tropospheric shear can modify those interactions. Recently, Stephan (2020) demonstrated how trapped gravity waves could modulate trade wind cumulus. Lane and Zhang (2011) showed that gravity waves and mesoscale cloud populations become dynamically coupled, with the gravity waves feeding back on the convective clouds through transient ascent and descent that modifies their morphology. Grant et al. (2018, 2020) demonstrated that when cold pools are weak, gravity waves can help maintain long-lived mesoscale systems. In this study, idealized simulations (similar in concept to Tulich

and Mapes 2008, Lane and Zhang 2011, LM15, Grant et al. 2018; 2020 and others) are used to further explore gravity wave-convection coupling.

The key element of this study exploits the fact that vertical wind shear affects the vertical propagation of gravity waves (e.g., Booker and Bretherton 1967), and changes in vertical propagation aloft can influence the underlying wave spectrum through ducting and reflection (e.g., Lindzen and Tung 1976). In the idealized experiments herein, the lower-stratospheric wind shear is altered to change the vertical propagation characteristics of gravity waves, which thereby modifies the characteristics of the tropospheric gravity waves without directly affecting the convection through advection by the mean flow. The approach provides focus on a previously unexplored aspect of stratosphere-troposphere interactions.

This study also has some relevance for the interaction between the Quasi-Biennial Oscillation (QBO) and the Madden-Julian Oscillation (MJO), which is receiving attention due to the impacts of the QBO on MJO predictability (e.g., Nishimoto and Yoden 2017, Lim et al. 2019). The QBO induces noteworthy variability in wind shear in the upper troposphere and lower stratosphere (UTLS) and recent idealized simulations (Martin et al. 2019) explored the roles of QBO-induced shear and stability on convection. Bui et al. (2017, 2019) produced a QBO-like oscillation in long-running idealized simulations, demonstrating modulation of the convection and shear by the oscillation. Those studies incorporate the influence of UTLS flow variations on the convection, whereas here only the influence of the lower-stratospheric shear is considered. This approach isolates the mechanisms associated with gravity waves from those related to advective process in troposphere. A number of previous studies have examined the role of gravity waves in contributing to the formation of the QBO (e.g., Piani et al. 2000); this is the first study to focus on the influence of QBO-like stratospheric shear on convection.

2 Methods

The idealized numerical model experiments use the nonhydrostatic and compressible CM1 model (Cloud Model 1 revision 15, Bryan and Fritsch 2002), with a similar configuration to LM15. The domain is a three-dimensional doubly-periodic channel with length (x-direction) 2040 km, width (y-direction) 120 km, and depth (z-direction) 40 km. The channel is long enough to permit multiple MCSs to exist simultaneously and deep enough to reduce any influence of the

upper boundary on the gravity wave-shear interactions. The horizontal grid spacing is 1 km; the vertical grid spacing is 100 m at the surface, increasing to 200 m for z>550 m. Physical parameterizations are the same as LM15 and described in the Supporting Information (text S1).

The model is initialized with the same sounding as LM15 (a tropical sounding observed near Darwin Australia during a period of intense island thunderstorms), except for z>16.5 km the Brunt-Väisälä frequency N is 0.02 s^{-1}. Convection is maintained via horizontally-uniform and constant-in-time cooling of 1.5 K day^{-1} from the surface to z =9.5 km. Between z =9.5 km and z =15.5 km the cooling decreases linearly with height and is zero above z =15.5 km. The lower-most boundary is a frictionless 300-K sea-surface with windspeed-dependent surface fluxes.

Most of the analyses focuses on a ~10-day period, 300-550 hours after model initialization, because during those times all simulations are dominated by propagating convective lines. This period offers the cleanest comparison between the two experiments because the convection is in a similar regime for a relatively long period. Although not shown, the mechanism explored in this manuscript is also present in later stages of this and similar simulations. Two specific simulations are: EX-CTRL (Experiment-Control), which has zero initial wind everywhere; and EX-SH (Experiment-Shear), which has zero initial wind in the troposphere and in the x-direction decreases linearly between z =15 and z =20 km to -25 m s^{-1} and is then constant aloft. The strength and magnitude of the wind shear is broadly consistent with those within the QBO (e.g., Piani et al. 2000). The Supporting Information contains profiles of the mean state (Fig. S1). The wind profiles can evolve with time, but there is little change between the initial profiles and those during the analysis period. The thermodynamic profiles also evolve in time, but do not vary significantly over the analysis period and are very similar for both experiments. The cooling profile leads to deep convection with cloud tops below approximately z =11 km. An important point for EX-SH is that the convective clouds never penetrate the shear layer, remaining at least 3 km below it. Thus, the shear cannot directly interact with the convective systems and any influence is indirect.

During the analysis period, model data are averaged in the y-direction and output every two minutes. These data are analyzed using 2D space (x) – time (t) spectral analysis. The power spectral density of the vertical velocity is calculated for z =5 km by averaging nine overlapping-

115 in-time spectra that are each 50 hours long. Before calculating each individual spectrum, a
116 cosine-taper window is applied in the time domain with tapering applied to the first and last 5
117 hours (10%) of each 50-hour series. For plotting, the final spectra are averaged in wavenumber-
118 frequency space using a 3 × 3 boxcar filter. For these spectra the sign of the horizontal
119 wavenumber, k, is the same as the horizontal phase speed, c, in the x-direction (defined as $c=\omega/k$,
120 where ω is the frequency).

121 **3 Model Results**

122 The two experiments contain similar cloud evolution (Fig. 1). Clouds develop after about 60
123 hours, initially featuring small cumulus that show no organization. Between 100 to 200 hours
124 propagating features emerge, though there is little change in the spatial scales of the clouds
125 compared to earlier. Between 200 to 250 hours, larger contiguous regions of clouds emerge,
126 associated with prominent v-shaped features (in x-t space) that have been identified in prior
127 studies to propagate slower than 10 m s^{-1} and be associated with cold pools (e.g., Grabowski and
128 Moncrieff 2001, Shige and Satomura 2001, Tulich and Mapes 2008, Lane and Zhang 2011, etc.).
129 After approximately 250 hours, mesoscale organization ensues: propagating convective systems
130 dominate the cloud field with increased intensity compared to earlier times. These propagating
131 MCSs last tens of hours, cover regions exceeding 100 km, and have typical propagation speeds
132 of 3-5 m s^{-1} in either direction. The propagation speed does vary, presumably related to the
133 strength of the cold pools and the degree of coupling with gravity waves. There is little change in
134 the convective regime for each experiment during the analysis period (300 to 550 hours) and the
135 domain-mean rain is approximately steady (not shown), making it an appropriate period of focus.
136 After about 600 hours (not shown), the convection continues to grow upscale to eventually form
137 a few larger clusters and the results are likely unduly influenced by the domain geometry; for this
138 reason, these later times are not considered.

139

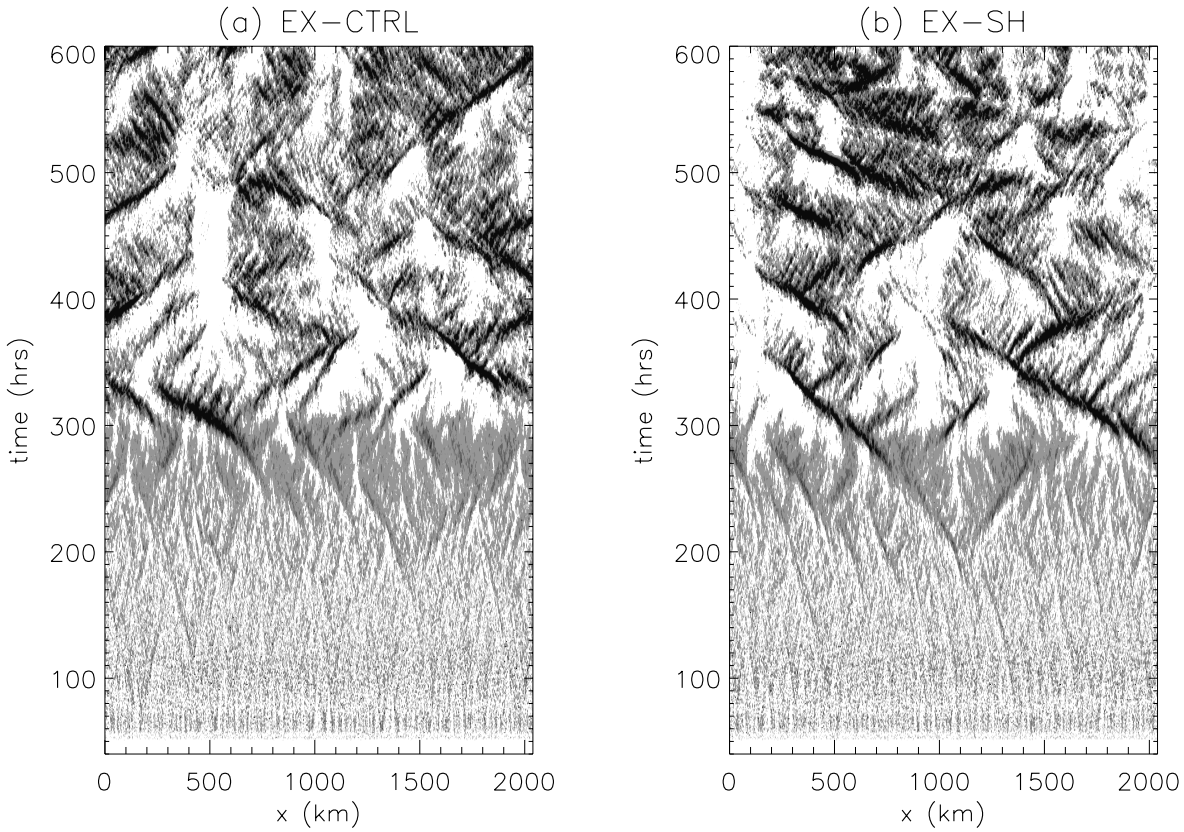

Figure 1. Time-distance diagrams of the *y*-average of the vertically-integrated total cloud (water and ice) mixing ratio for **a** EX-CTRL and **b** EX-SH. Shading intervals are 0.05, 0.2, 0.4, 0.6 g kg^{-1}km, with dark shading representing larger values.

Although there are similarities in the evolution of the cloud populations in the two experiments, inspection of the MCS propagation characteristics reveals important differences between EX-CTRL and EX-SH. For EX-CTRL (Fig. 1a) the MCSs show no preferred direction of propagation and there is approximately an equal number of systems propagating in the positive and negative *x*-directions. For EX-SH (Fig. 1b), however, there is a distinct preference for MCSs propagating in the negative *x*-direction. There are MCSs propagating in the positive *x*-direction, but these are fewer, generally weaker and shorter lived compared to those propagating in the negative *x*-direction. These differences between the two experiments are also demonstrated more

quantitatively in the Supporting Information (Fig. S2), highlighting that the largest difference is for systems propagating in the negative x-direction at approximately 3.5 m s^{-1}.

The domain-mean rainfall is approximately the same in the two experiments for the analysis period (EX-CTRL: 2.3 mm/day, EX-SH: 2.4 mm/day), owing to the constraints placed by the constant tropospheric cooling. However, there are differences in the spatial distribution of rainfall between the two experiments, with EX-SH producing larger values of maximum mesoscale rainfall and smaller values of minimum mesoscale rainfall. Here, mesoscale rainfall is defined as the hourly rainfall accumulation averaged over 120×120 km areas (calculated at each grid point in the x-direction). The temporal mean of the maximum mesoscale rainfall is 8.9 mm/day for EX-CTRL and 10.1 mm/day for EX-SH. The temporal mean of the minimum mesoscale rainfall is 0.07 mm/day for EX-CTRL and 0.013 mm/day for EX-SH. Thus, EX-SH features mesoscale regions of stronger rain than EX-CTRL and, consistent with the similar domain mean rainfall, EX-SH features mesoscale areas that are drier than EX-CTRL. EX-SH also has slightly larger domain-mean upper-level cloud amounts compared to EX-CTRL (see Supporting Information Fig. S1b).

The inclusion of lower-stratospheric shear has led to noteworthy differences in the organizational characteristics of the simulated convection. The propagating MCSs show a preference to propagate in the same direction as the lower-stratospheric shear vector (i.e., *downshear*) at the expense of MCSs propagating in the opposite direction to the lower-stratospheric shear (i.e., *upshear*). The simulation without mean shear shows no preference for the direction of MCS propagation. The change in the characteristics of the MCSs in EX-SH also leads to increased cloud amounts and mesoscale rainfall intensity. These sensitivities to lower-stratospheric shear are robust, extending to other simulations with different lower-stratospheric shear profiles (see Supporting information Fig. S4). In the next section spectral analysis is used to expose the mechanisms influencing the sensitivity to lower-stratospheric shear.

4 Gravity waves

The spectrum of the 5-km vertical velocity (Fig. 2) is used to identify the characteristics of the tropospheric gravity waves that are generated by and interact with the convective clouds. This spectrum includes signals from gravity waves and convective updrafts and downdrafts, which are

intertwined and practically inseparable. Here z=5 km is chosen as it represents an altitude where moderately deep clouds and gravity waves coexist and interact.

EX-CTRL (Fig. 2a) features a spectrum that is almost exactly symmetric about k=0, because the mean wind is zero. The spectrum features local maxima in power that follow curved paths, which correspond closely to lines of constant vertical wavelength, λ_z (where $\lambda_z=2\pi/m$ and m is the vertical wavenumber). Here λ_z is defined by the non-hydrostatic gravity wave dispersion relation (with no mean wind), $m^2=k^2N^2/\omega^2-k^2$. Lines with λ_z equal to 4, 8, and 16 km are shown, determined using N=0.011 s^{-1} (its value at z=5 km). The strong agreement between maxima in the spectra and the dispersion curves suggests that much of the variability in vertical velocity is consistent with gravity waves.

Tropospheric gravity waves with similar vertical wavelengths to those above have been shown to be important for gravity wave-convection coupling, which occurs because the wave-induced ascent can destabilize the environment surrounding convection and also modulate the convective cloud population. For example, in idealized simulations similar to those here, Lane and Zhang (2011) identified coupling between convection and waves with λ_z=10 km, and Tulich and Mapes (2008) highlighted the importance of short vertical wavelength gravity waves, termed ‘gust front modes’. These two studies also demonstrate how such tropospheric waves are generated as a response to the evaporative cooling associated with precipitation. Further, evidence of the importance of waves with 4 and 8 km vertical wavelengths, is found in the Supporting Information (Text S2 and Fig. S3), which shows how these modes explain much of the mesoscale cloud variability.

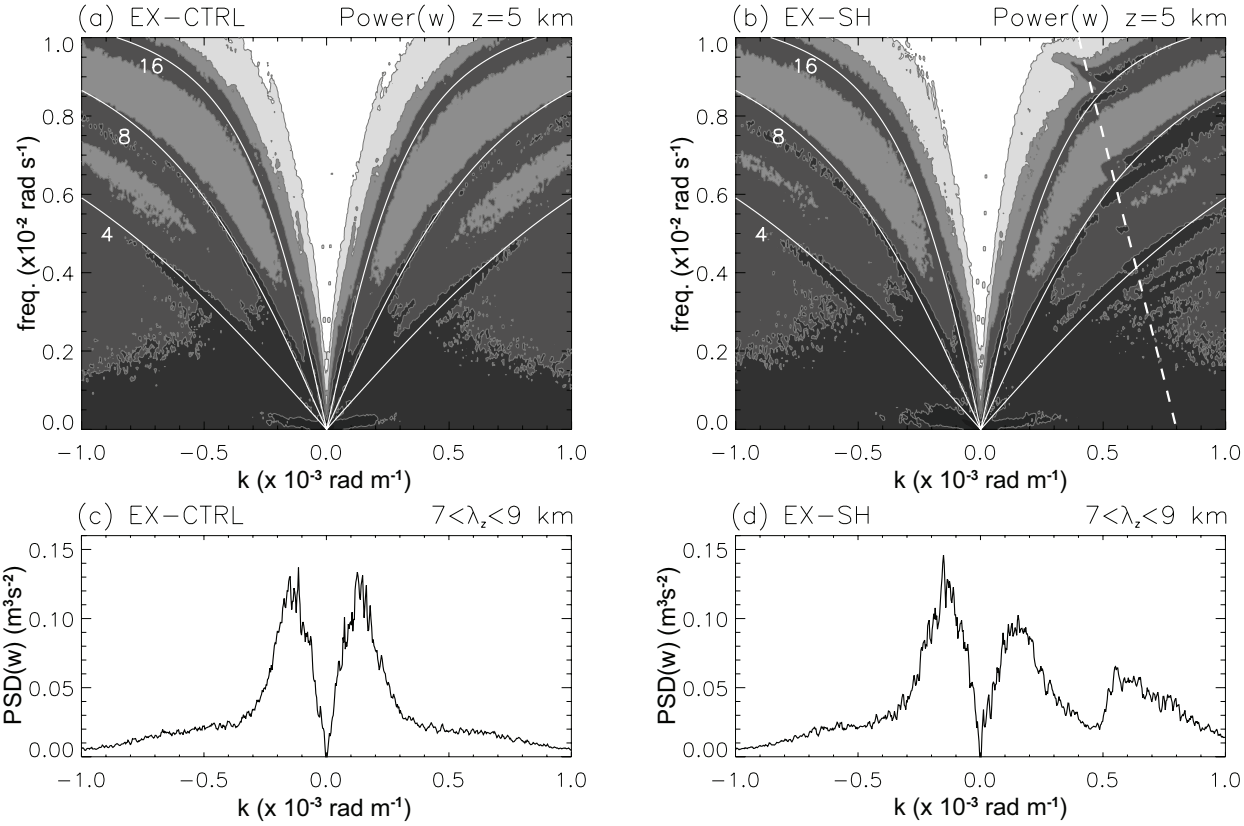

Figure 2. Power spectra of the (*y*-averaged) vertical velocity at z =5 km for **a**,**c** EX-CTRL and **b**,**d** EX-SH. **a**,**b** are the 2D (k-ω) spectra, normalized to the maximum value of the spectrum in **b**. Shading is at 10^{-6}, 10^{-5},…,10^{-2} intervals with dark shading representing largest values. Thin white lines correspond to solutions of the non-hydrostatic gravity wave dispersion relation for vertical wavelengths, λ_z, of 4, 8, and 16 km (as labelled); the thick dashed white line in **b** is defined in the text. **c**,**d** are the corresponding power spectral densities (PSD), filtered for $7<\lambda_z<9$ km.

The spectrum for EX-SH (Fig. 2b) has similarities and important differences to EX-CTRL. As for EX-CTRL, EX-SH features local maxima in power that follow the same dispersion relation curves. For $k<0$ the spectrum is very similar to EX-CTRL. For $k>0$ at small wavenumbers/frequencies the power also follows the dispersion curves, but at larger wavenumbers/frequencies this pattern is disrupted. The spectral boundary of this disruption is well identified by the overlaid dotted line (defined below). The differences in the spectrum between the two experiments is highlighted in Figs. 2c-d, which shows the power that falls along the spectral region defined by λ_z=8±1 km. (This spectral range is chosen as it corresponds to one of the prominent signals in Fig. 2 a-b). Here, comparison of Figs. 2c and 2d identifies that for this wave mode negative phase speeds ($k<0$) are unaffected by the shear layer aloft. In contrast,

for positive phase speeds ($k>0$), for EX-SH there is a decrease in power at smaller wavenumbers and an increase in power for the larger wavenumbers compared to EX-CTRL.

The overlaid dotted line in Fig. 2b is defined by $\omega=N_s+U_s k$, where U_s =-25 m s^{-1} is the stratospheric wind at the top of the shear layer and N_s=0.02 s^{-1} is the stratospheric Brunt-Väisälä frequency. Linear theory says that vertically-propagating gravity waves will become evanescent if the magnitude of the intrinsic frequency (defined as $\hat{\omega}=\omega-Uk$, where U is the component of the mean wind in the direction of wave propagation) exceeds the local Brunt-Väisälä frequency. When upward-propagating waves become evanescent they can be reflected downwards. Thus, $\omega=N_s+U_s k$ in Fig. 2b identifies frequencies where $\hat{\omega}=N$ at (or above) the top of the shear layer; upward-propagating waves with frequencies/wavenumbers to the right of the line would all become evanescent by the top of the shear layer. Waves with frequencies/wavenumbers farthest from the line (but still to the right of it) would become evanescent in the lower parts of the shear layer and those closer to the line would become evanescent in the upper parts of the shear layer (see Lane and Clark 2002 for a detailed discussion of this mechanism). As the spectra in Fig. 2 are at z=5 km, i.e., well below the shear layer, it can be concluded that the disruption to the spectrum at this altitude is a manifestation of the waves being reflected downwards from farther aloft. This reflection only occurs for waves propagating in the positive direction, i.e., opposite to the lower-stratospheric shear vector, and the occurrence of this reflection is well explained by linear theory.

It is worth noting that a large part of the wave spectrum interacts with a critical level (U-c=0, where U is the mean wind in the x-direction) in the shear layer in EX-SH (for k<0). However, there is no evidence of reflection downward from this critical level as the 5-km wave spectrum is almost identical for EX-CTRL and EX-SH for $k<0$. Thus, unlike Shige and Satomura (2001), who demonstrated an important role of a tropospheric critical level in their convective morphology, the stratospheric critical level here has an undetectable influence on the tropospheric waves.

5 Discussion

Lower-stratospheric shear is shown to influence the mesoscale organization of convection. This influence is not through direct (advective) interactions between the convection and the shear

because the shear is well above the convection. Instead, the lower-stratospheric shear influences the tropospheric velocities by reflecting upward-propagating gravity waves downwards. The reflection affects the tropospheric gravity wave modes, as demonstrated in Fig. 2, which are linked to the organization of convection. Here the lower-stratospheric shear-driven reflection only occurs for waves propagating in the opposite direction to the shear vector (i.e., upshear), creating ubiquitous asymmetry in the tropospheric gravity wave field.

How does the asymmetric tropospheric gravity wave field lead to a preferred propagation direction for the MCSs? Consider two sections of the *y*-averaged vertical velocity from EX-SH for representative systems: one propagating in the negative direction (downshear with respect to the lower-stratospheric shear) (at 330 hrs Fig. 3a) and one propagating in the positive *x*-direction (upshear with respect to the lower-stratospheric shear) (at 360 hours Fig. 3b). These two systems occur close to each other in space and time, yet as is typical, the downshear system is more intense and long-lived than the upshear system (cf. Fig. 1). The vertical velocity in Fig. 3a identifies a coherent set of gravity waves ahead of the downshear-propagating storm, which are identified as wave-like signals in the vertical velocity with tilted phase lines. Coinciding with these waves, the surface-based convective available potential energy (CAPE, calculated from the *y*-average of relevant thermodynamic variables, Fig. 3c) is enhanced ahead of the storm, implying that the waves have a destabilizing influence on the storm environment. The local maxima in CAPE ahead of the storm (e.g., at $x \approx 283$, 313, 330 km) correspond with coherent regions of gravity wave ascent, in the lower troposphere (i.e., $x \approx 283$, 330 km) or middle-to-upper troposphere (i.e., at $x \approx 313$ km). In contrast, the tropospheric vertical velocity ahead of the upshear-propagating systems (Fig. 3b) features a less coherent pattern, with evidence of interference between upward-propagating and downward-reflected waves (creating a crossed pattern in the vertical velocity). Presumably, the interference and lack of coherence reduces the destabilizing influence of the tropospheric waves, and the CAPE perturbations (Fig. 3d) ahead of the storm are much weaker and it is difficult to link them to the gravity waves. Note that within the storms the CAPE values are different for the two cases, likely related to different stages of convective lifecycle. As shown in the Supporting Information (Text S4 and Fig. S5), these examples are representative of the key processes because all downshear-propagating storms in EX-SH feature stronger CAPE perturbations ahead of them compared to upshear-propagating

storms. Moreover, in EX-CTRL there is no systematic asymmetry in the strength of CAPE perturbations ahead of storms propagating in the positive or negative *x*-directions.

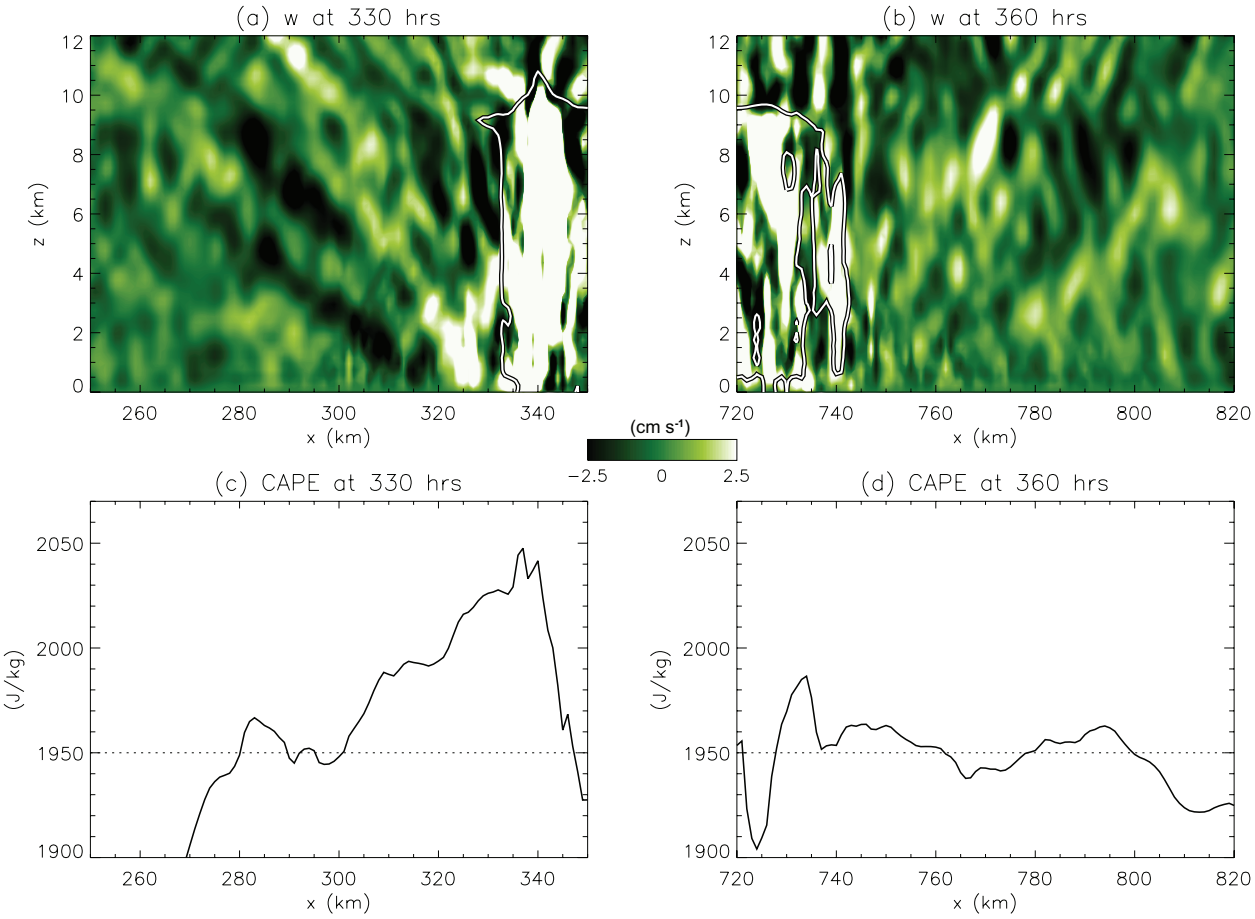

Figure 3. Selected locations in EX-SH at (**a**,**c**) 330 and (**b**,**d**) 360 hours. (**a**,**b**) Cross-sections of the *y*-averaged vertical velocity (green shading) and the total cloud plus rainwater mixing ratio (black/white line contoured at 0.05 g kg^{-1}). (**c**,**d**) the corresponding values of CAPE, with the dotted line included to aid comparison. See Supporting Information Fig. S5 for the section locations.

The above analysis suggests that the preference for convective systems to propagate downshear is actually related to the suppression of upshear-propagating convective systems. The lower-stratospheric shear causes a reflection of upshear-propagating gravity waves back into the troposphere, reducing the coherence of the tropospheric gravity wave field and disrupting the destabilizing influence of the tropospheric gravity waves ahead of the convection. The gravity waves are unaffected for those waves (and systems) propagating downshear and for situations

without stratospheric shear. The close similarity in the power spectra for $k<0$ for the two experiments (cf. Figs. 2c-d) provides supporting evidence. Moreover, the weakening of the spectral power for low wavenumber signals for $k>0$ in EX-SH compared to EX-CTRL, is also consistent with a suppression of the upshear-propagating convection.

6 Conclusions

This study has identified a subtle but robust influence of lower-stratospheric wind shear on the mesoscale organization of convection. The underlying mechanism is caused by gravity waves, which are known to become dynamically coupled to convective clouds. The lower-stratospheric shear affects the organization by changing the ability of gravity waves to propagate into the stratosphere, causing part of the wave spectrum to be reflected back into the troposphere. This wave reflection reduces the coherence of the tropospheric waves and disrupts their ability to destabilize the environment and promote convection. As explained by gravity wave theory, this wave reflection only occurs for waves propagating in the opposite direction to the lower-stratospheric shear, thereby reducing the occurrence, strength and longevity of convective storms propagating in this direction. The result is a preference for long-lived MCSs that propagate in the same direction as the lower-stratospheric shear. Previous studies have explored the influence of tropospheric shear on gravity wave-convection interactions and convective organization, but this is the first study to isolate the influence of stratospheric shear on convective organization.

As is well known, lower-tropospheric wind shear has an important influence on mesoscale organization through direct interactions with cold pools, and tropospheric shear also affects organizational characteristics through differential advection and influence on storm tilt. The effect of stratospheric shear on tropospheric convection represents a new paradigm for convective organization. As shown here, the lower-stratospheric shear will favor downshear-propagating systems and lower-tropospheric shear commonly favors downshear-propagating systems too; thus, situations in unidirectional shear may allow the two mechanisms to work in concert. It is likely that the lower-stratospheric shear may be most important when gravity waves dominate convective organization, such as if the tropospheric shear or cold pools are weak. Such conditions occur in the tropics, and the lower-stratospheric shear considered here is similar to that within the QBO. In the midlatitudes, lower-stratospheric shears like those here are common,

but tropospheric shear is typically also strong and likely dominates the organizational process. Further work exploring the relative and combined influences of tropospheric and stratospheric shear on convective organization should be a topic for future research.

These results demonstrate unequivocally that gravity waves play an important role in mesoscale organization. There have been many studies that have explored convection-gravity wave interactions, but typically it has been difficult to separate the specific role of the gravity waves on the convection because they are intertwined and inseparable. This study has developed a framework whereby the change in shear adjusts the vertical propagation of gravity waves through the lower stratosphere, hence modifying the characteristics of the tropospheric waves without changing the tropospheric background state and impacting the convection directly. The impacts on convection here are only related to gravity waves, providing perhaps the most convincing evidence to date of the existence of gravity wave-convection coupling.

Now consider stratosphere-troposphere interactions and the potential role of stratospheric shear associated with the QBO on convection. These results suggest that westward-propagating MCSs might be preferred during easterly phases of the QBO (and vice-versa). It is typical for westward-propagating MCSs to be embedded within the MJO (e.g., Tulich and Kiladis 2012), so it is plausible that this mechanism for stratospheric shear / convection interactions could contribute to the link between the MJO and easterly phases of the QBO. However, recent idealized modelling work (Martin et al. 2019) suggests that the QBO-induced temperature perturbations in the upper-troposphere may be more important than shear. Of course, in reality the QBO-induced shears do penetrate the upper-troposphere, allowing them to directly impact the convective structures (unlike the mechanism here). Nonetheless, the impact of the stratosphere (and the QBO) on tropospheric gravity waves and mesoscale gravity wave-convection coupling might still have some relevance.

The influence of lower-stratospheric shear on convective organization highlights the importance of realistic representation of gravity wave-shear interactions in simulating mesoscale organization, especially in the convection-permitting models that are prevalent in operational weather prediction and regional climate modeling. Such models typically have coarse vertical resolution in the UTLS and absorbing layers in the lower stratosphere. It is likely that they do not

always provide a realistic representation of the propagation and reflection of mesoscale gravity waves in the UTLS, which may unduly affect their ability to represent organized convection realistically. These mechanisms are also unable to be represented in global models with parameterized convection. Further consideration of these points is warranted.

In summary, this work has identified a new paradigm explaining aspects of convective organization, whereby the lower-stratospheric wind shear can influence the morphology of mesoscale convection. A key element of this process is the coupling between gravity waves and convection. These results have important implications for improved understanding of organized convection, stratosphere-troposphere interactions and numerical modeling of storms. Of course, these results are derived from idealized numerical experiments and it is unclear how important this mechanism is in the real world. Further exploration of the mechanism in observational data and more realistic simulations should be a topic of continuing research.

Acknowledgments

This work was supported by the Australian Research Council's Centres of Excellence program (CE170100023). Computational resources were provided by the National Computational Infrastructure Facility (NCI). Thank you to George Bryan for making the CM1 model available and providing ongoing support for its use, and Stefan Tulich for providing the autocorrelation code used to create Fig. S2. Thank you also to Shigeo Yoden, Claudia Stephan and two anonymous reviewers for their comments that helped improve the manuscript, and to Alvin Stone and Karla Fallon for help with the plain language summary. This work benefited from many discussions with my friend and collaborator Prof. Fuqing Zhang (dec.), with this work being spawned from our previous collaboration on this topic.

Data Availability

CM1 is an open source model developed and maintained by Dr George Bryan from the National Center for Atmospheric Research. The model code (for revision 15) can be downloaded here: http://www2.mmm.ucar.edu/people/bryan/cm1/downloadcode.html . The model output data

379 used for the figures and analysis in this paper can be downloaded here:

380 https://doi.org/10.6084/m9.figshare.12955187

381

References

Booker, J., & Bretherton, F., 1967: The critical layer for internal gravity waves in a shear flow. *Journal of Fluid Mechanics,* **27**, 513-539. doi:10.1017/S0022112067000515

Bryan, G. H., and J. M. Fritsch, 2002: A Benchmark Simulation for Moist Nonhydrostatic Numerical Models. *Mon. Wea. Rev.*, **130**, 2917–2928, https://doi.org/10.1175/1520-0493(2002)130<2917:ABSFMN>2.0.CO;2.

Bui, H., E. Nishimoto, and S. Yoden, 2017: Downward Influence of QBO-Like Oscillation on Moist Convection in a Two-Dimensional Minimal Model Framework. *J. Atmos. Sci.*, **74**, 3635–3655, https://doi.org/10.1175/JAS-D-17-0095.1.

Bui, H., Yoden, S., and Nishimoto, E., 2019: QBO-like oscillation in a three-dimensional minimal model framework of the stratosphere–troposphere coupled system. *SOLA*, **15**, 62-67. https://doi.org/10.2151/sola.2019-013

Fovell, R.G., 2002: Upstream influence of numerically simulated squall-line storms. *Q.J.R. Meteorol. Soc.*, **128**, 893-912. doi:10.1256/0035900021643737

Grabowski, W.W. and Moncrieff, M.W., 2001: Large-scale organization of tropical convection in two-dimensional explicit numerical simulations. *Q.J.R. Meteorol. Soc.*, **127**, 445-468. doi:10.1002/qj.49712757211

Grant, L. D., T. P. Lane, and S. C. van den Heever, 2018: The Role of Cold Pools in Tropical Oceanic Convective Systems. *J. Atmos. Sci.*, **75**, 2615–2634, https://doi.org/10.1175/JAS-D-17-0352.1.

Grant, L. D., Moncrieff, M. W., Lane, T. P., & van den Heever, S. C., 2020: Shear-parallel tropical convective systems: Importance of cold pools and wind shear. *Geophysical Research Letters*, **47**, e2020GL087720. https://doi.org/10.1029/2020GL087720

Houze, R. A., Jr., 2018: 100 years of research on mesoscale convective systems. *Meteorological Monographs*, **59**, 17.1–17.54, https://doi.org/10.1175/AMSMONOGRAPHS-D-18-0001.1.

Lac, C., J. Lafore, and J. Redelsperger, 2002: Role of Gravity Waves in Triggering Deep Convection during TOGA COARE. *J. Atmos. Sci.*, **59**, 1293–1316, https://doi.org/10.1175/1520-0469(2002)059<1293:ROGWIT>2.0.CO;2.

Lane., T.P. and Clark, T.L., 2002: Gravity waves generated by the dry convective boundary layer: Two-dimensional scale selection and boundary-layer feedback. *Quart. J. Roy. Meteor. Soc.*, **128**, 1543-1570. https://doi.org/10.1002/qj.200212858308

Lane, T. P., and M. W. Moncrieff, 2015: Long-Lived Mesoscale Systems in a Low–Convective Inhibition Environment. Part I: Upshear Propagation. *J. Atmos. Sci.*, **72**, 4297–4318, https://doi.org/10.1175/JAS-D-15-0073.1.

Lane, T. P., and M. J. Reeder, 2001: Convectively Generated Gravity Waves and Their Effect on the Cloud Environment. *J. Atmos. Sci.*, **58**, 2427–2440, https://doi.org/10.1175/1520-0469(2001)058<2427:CGGWAT>2.0.CO;2.

Lane, T. P., and F. Zhang, 2011: Coupling between Gravity Waves and Tropical Convection at Mesoscales. *J. Atmos. Sci.*, **68**, 2582–2598, https://doi.org/10.1175/2011JAS3577.1.

LeMone, M. A., Zipser, E. J., & Trier, S. B., 1998: The role of environmental shear and thermodynamic conditions in determining the structure and evolution of mesoscale convective systems during TOGA COARE. *J. Atmos. Sci.*, **55**, 3493–3518. https://doi.org/10.1175/1520-0469(1998)055<3493:TROESA>2.0.CO;2

Lim, Y., Son, S., Marshall, A.G., Hendon, H.H., and Seo, K.-H., 2019: Influence of the QBO on MJO prediction skill in the subseasonal-to-seasonal prediction models. *Clim Dynamics,* **53,** 1681–1695. https://doi.org/10.1007/s00382-019-04719-y

Lindzen, R. S., & Tung, K., 1976: Banded Convective Activity and Ducted Gravity Waves, *Mon. Wea. Rev.*, **104**, 1602-1617. https://doi.org/10.1175/1520-0493(1976)104<1602:BCAADG>2.0.CO;2

Mapes, B. E., 1993: Gregarious Tropical Convection. *J. Atmos. Sci.*, **50**, 2026–2037, https://doi.org/10.1175/1520-0469(1993)050<2026:GTC>2.0.CO;2.

Martin, Z., S. Wang, J. Nie, and A. Sobel, 2019: The Impact of the QBO on MJO Convection in Cloud-Resolving Simulations. *J. Atmos. Sci.*, **76**, 669–688, https://doi.org/10.1175/JAS-D-18-0179.1.

Moncrieff, M. W., 1981: A theory of organized steady convection and its transport properties. *Quart. J. Roy. Meteor. Soc.*, **107**, 29–50. https://doi.org/10.1256/smsqj.45102

Moncrieff, M. W., Liu, C., & Bogenschutz, P., 2017: Simulation, Modeling, and Dynamically Based Parameterization of Organized Tropical Convection for Global Climate Models, *J. Atmos. Sci.*, **74**, 1363-1380. https://doi.org/10.1175/JAS-D-16-0166.1

Nishimoto, E., and S. Yoden, 2017: Influence of the Stratospheric Quasi-Biennial Oscillation on the Madden–Julian Oscillation during Austral Summer. *J. Atmos. Sci.*, **74**, 1105–1125, https://doi.org/10.1175/JAS-D-16-0205.1.

Parker, M. D., , and R. H. Johnson, 2000: Organizational modes of midlatitude mesoscale convective systems. *Mon. Wea. Rev*, **128 ,** 3413–3436. https://doi.org/10.1175/1520-0493(2001)129<3413:OMOMMC>2.0.CO;2

Piani, C., D. Durran, M. J. Alexander, and J. R. Holton, 2000: A Numerical Study of Three-Dimensional Gravity Waves Triggered by Deep Tropical Convection and Their Role in the Dynamics of the QBO. *J. Atmos. Sci.*, **57**, 3689–3702, https://doi.org/10.1175/1520-0469(2000)057<3689:ANSOTD>2.0.CO;2.

Shige, S., and T. Satomura, 2001: Westward Generation of Eastward-Moving Tropical Convective Bands in TOGA COARE. *J. Atmos. Sci.*, **58**, 3724–3740, https://doi.org/10.1175/1520-0469(2001)058<3724:WGOEMT>2.0.CO;2.

Stechmann, S. N., and A. J. Majda, 2009: Gravity Waves in Shear and Implications for Organized Convection. *J. Atmos. Sci.*, **66**, 2579–2599, https://doi.org/10.1175/2009JAS2976.1.

Stephan, C. C., 2020: Seasonal Modulation of Trapped Gravity Waves and Their Imprints on Trade Wind Clouds. *J. Atmos. Sci.*, **77**, 2993–3009, https://doi.org/10.1175/JAS-D-19-0325.1.

Thorpe, A.J., Miller, M.J. and Moncrieff, M.W., 1982: Two-dimensional convection in non-constant shear: A model of mid-latitude squall lines. *Q.J.R. Meteorol. Soc.*, **108**, 739-762. doi:10.1002/qj.49710845802

Tulich, S. N., and G. N. Kiladis, 2012: Squall Lines and Convectively Coupled Gravity Waves in the Tropics: Why Do Most Cloud Systems Propagate Westward? *J. Atmos. Sci.*, **69**, 2995–3012, https://doi.org/10.1175/JAS-D-11-0297.1.

Tulich, S. N., and B. E. Mapes, 2008: Multiscale Convective Wave Disturbances in the Tropics: Insights from a Two-Dimensional Cloud-Resolving Model. *J. Atmos. Sci.*, **65**, 140–155, https://doi.org/10.1175/2007JAS2353.1.

Weisman, M. L., and R. Rotunno, 2004: "A Theory for Strong Long-Lived Squall Lines" Revisited. *J. Atmos. Sci.*, **61**, 361–382, https://doi.org/10.1175/1520-0469(2004)061<0361:ATFSLS>2.0.CO;2.

References for Supporting Information

Lin, Y.-L., R. D. Farley, , and H. D. Orville, 1983: Bulk parameterization of the snow field in a cloud model. *J. Climate Appl. Meteor.*, **22**, 1065–1092, doi:10.1175/1520-0450(1983)022<1065:BPOTSF>2.0.CO;2.

Rotunno, R., , and K. A. Emanuel, 1987: An air–sea interaction theory for tropical cyclones. Part II: Evolutionary study using a nonhydrostatic axisymmetric numerical model. *J. Atmos. Sci.*, **44**, 542–561, doi:10.1175/1520-0469(1987)044<0542:AAITFT>2.0.CO;2.